Multimedia Tools and Applications (2019) 78:25241–25258
https://doi.org/10.1007/s11042-019-07744-5

Adaptive gamma correction for contrast enhancement of remote sensing images

Shubhi Kansal[1] · **Rajiv Kumar Tripathi**[1]

Received: 7 August 2018 / Revised: 2 April 2019 / Accepted: 9 May 2019 /
Published online: 23 May 2019

Abstract
Contrast magnification is a critical parameter of image enhancement. Remote sensing images are distance captured images, so they naturally have very low contrast as compared to other images. In this paper a very simple and efficient technique based on adaptive gamma correction and Discrete cosine transform(DCT) is proposed which can bring out the maximum information present in the image and enhance the contrast of the image very well. We first apply an adaptive gamma correction which enhances the image globally and than high frequency components of DCT transformation are further altered to intensify the minute details of the image. Proposed method is judged on the basis of visual quality and numerical parameters compared with the other existing techniques. The results obtained for proposed technique surpasses all the other methods both qualitatively and quantitatively.

Keywords Gamma correction · DCT transformation · Enhancement

1 Introduction

For many years, remote sensing images represented a major role in the field of land cultivation, military, historical surveying, calamity monitoring, coastal land use and regulation etc [3–5, 14]. The contrast of the remote sensing images is destroyed due to its distant capture and also due to the environmental conditions. Hence, an efficient technique is required which can enhance the contrast as well as brings out the minute details of the remote sensing images.

Histogram equalization (HE) is generally used due to its simple and efficient approach for image enhancement. In HE, the contrast of the image is increased by taking transformation function as cumulative density function (CDF) of the image. However, there are some drawbacks when HE is applied. The image mean brightness is disturbed and the image is over enhanced.

In 2010, another method called as Satellite image contrast enhancement using discrete wavelet transform and regular value decomposition (SEDWT-SVD) [6] was proposed for

✉ Shubhi Kansal
kansalshubhi@yahoo.com

[1] National Institute of Technology, Delhi, 110040, India

the enhancement of the remote sensing images. This method belongs to the transform - domain method which divided the given image into the DWT subbands, and the image brightness was maintained by the singular value decomposition. The limitation of this method was that the overall information content of the image was less.

In 2013, Low contrast satellite images enhancement using discrete cosine transform pyramid and singular value decomposition (DCTPSVD) [2] was proposed. In this method the DCT high frequency coefficients of the image were divided into low sub-band and reverse L-shape block and than SVD was applied for image contrast enhancement purpose. This method suffered from halo artefacts and artificial noise in some of the images.

Again in 2013, another method was proposed for enhancing remote sensing images using dominant brightness level and adaptive intensity transformation [15]. This method, first calculated the brightness-adaptive intensity transfer functions in wavelet domain and than transformed the intensity values according to that function. Though this method preserved the brightness of the image but it introduced harsh noise in the images.

Adaptive gamma correction with weighting distribution (AGCWD) was proposed in 2013 [9]. In this method the gamma value was calculated using weighted histogram. AGCWD generated contrast enhancement results that preserved the overall brightness of an image, but the information contained in the brighter regions of the image was lost.

Regularized- histogram equalization and the discrete cosine transform (RHEDCT) [7] proposed in 2015 used both global and local contrast enhancement process. In this method the image histogram was altered by applying sigmoid function for global enhancement and than DCT was applied for local details enhancement. This method enhanced the images well but also introduced noise in the images.

In 2016, an adaptive gamma correction (AGC) for image enhancement was proposed [19]. It basically classified the images based on their statistical information and the parameters of AGC were set dynamically according to the image information. This method failed to preserve the edge details of the image.

Another method, using singular value decomposition (SVD) and AGC [12] was proposed for enhancement of computed tomography (CT) scan images. This method used discrete wavelet transform with SVD (DWT-SVD) followed by AGC for the contrast enhancement. The images generated by this method were not visually appealing.

Recently, a particle swarm optimization based contrast enhancement algorithm was proposed for gray scale images [13]. This method also employed gamma correction for image enhancement and the optimal gamma value was find using particle swarm optimization. This method has high computational complexity due to convergence.

An adaptive cuckoo search algorithm based satellite image enhancement technique was proposed in 2017 [22]. It comprised of a chaotic initialization phase which avoided the early convergence stage of an image. Secondly, an adaptive Lévy flight strategy was adopted to improve the convergence rate and finally a mutative randomization phase was included to achieve proper balance between exploration and exploitation phases. The computational complexity of this method is very high due to the three different phases which makes it unsuitable to be used in real time applications.

An optimally weighted piecewise gamma corrected method was proposed for satellite image enhancement [20]. In this method optimally ordered fractional differential (FD) unsharp masking and piece wise gamma correction was employed for the image contrast enhancement. Though this method provided good results but, it is very slow and very difficult to be used in real time applications.

A slantlet filter-bank based method was proposed for satellite image enhancement [21]. In this particular method auto-knee transfer function and gamma correction were applied using slantlet transform for enhancing the images. Since, filter is utilized in this method the number of calculations increased and the complexity also increased.

Recently, an efficient contrast enhancement method for remote sensing images (HCTLS) was proposed [16]. This particular method used histogram compacting transform and linear stretching for the enhancement of remote sensing images. The method although maintained the robustness but, it failed to bring out the maximum details of the image.

In this letter, a new contrast enhancement technique for remote sensing images is proposed to refine the overall contrast of the image as well as enhance the minute details of the image. We first apply a new adaptive gamma correction technique based on adaptive gamma correction (AGC) for global contrast enhancement of the image. Next, we apply DCT transformation on the gamma corrected image and higher frequency coefficients are altered in order to enhance the minute details of the image. After rigorous experiments on the different images the proposed technique outperformed state of the art methods qualitatively as well as quantitatively.

2 Motivation

The idea behind introducing this method is to enhance the complete image as well as enhance the local details of the image. As discussed in the introduction section all the state of the art methods have some or the other limitations associated with them such as:

- Shifting of mean brightness and over enhancement of an image.
- Very less enhancement of image details.
- Presence of halo artefacts, harsh noise and artificial noise in an image.
- Loss of information in the brighter portion of an image.
- Loss of edge details of an image.
- Increased complexity of the system due to large number of calculations.

The proposed technique can resolve these issues and gives high contrast image which can be further visualized in results section.

In this paper gamma correction is combined with DCT, the idea behind combining these two techniques can be observed from the following figures: Figures 1 and 2 shows the result of two remote sensing images for different conditions.

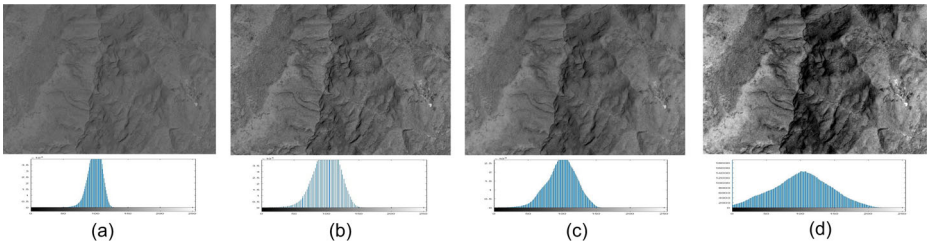

Fig. 1 GF-1 image: **a** Original **b** Enhancement with only gamma correction **c** Enhancement with only DCT adjustment **d** Enhancement with the proposed method

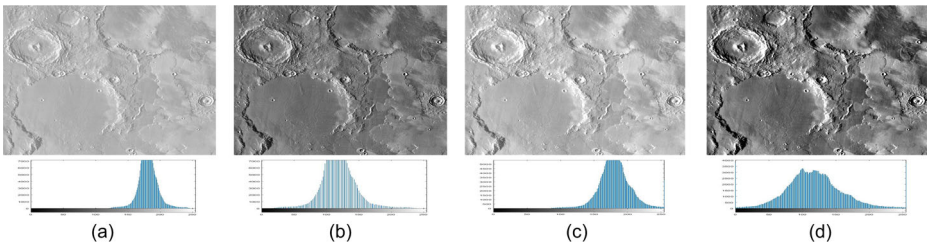

Fig. 2 Mars image: **a** Original **b** Enhancement with only gamma correction **c** Enhancement with only DCT adjustment **d** Enhancement with the proposed method

Figure 1 shows the GF-1 image. Figure 1a is the original image with its histogram. Figure 1b shows the resultant image with only gamma correction. As it can be observed that image is globally enhanced and histogram is stretched in comparison to original histogram. Figure 1c shows the resultant image with only DCT adjustment. It can be seen that local details are highlighted in this image. Also if we look at the histogram, it has sharp stretching. Figure 1d shows the resultant image with proposed method. As it can be clearly seen that this image is very well enhanced with both global and local features enhancement. Also histogram of this image covers the entire range of the pixel intensity. Similarly, Fig. 2 can also be analysed.

Hence, this was the motivation behind proposing this method.

3 Proposed method

Figure 3 shows the flowchart of the proposed method.

3.1 Enhancing the image globally by applying adaptive gamma correction

Let us consider an input remote sensing image I which is having a size X x Y with the intensity levels between 0 to L-1 $(I_0, I_1, ...I_i ..., I_{L-1})$ where L is the maximum number of grey levels. Let I_{max} and I_{min} represent the maximum and minimum intensity of image respectively. The proposed transformation function based on gamma correction is given as:

$$I_{out} = (I_k - I_{min})^{\gamma} \tag{1}$$

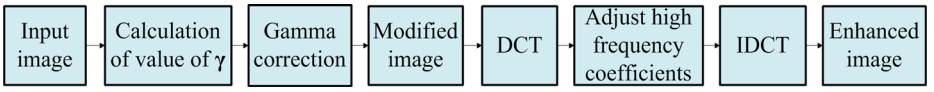

Fig. 3 Block diagram of proposed method

where I_{out} is the output enhanced image and I_k is the k^{th} intensity of the image. The value of γ is calculated as:

$$\gamma = \frac{log(L)}{log(I_{max} - I_{min})} \tag{2}$$

Since, this value of γ will change for every image , so it is adaptive in nature.

3.2 Detail enhancement by applying DCT

After the contrast of the image enhanced globally by the above procedure, we apply DCT transformation to further enhance the minute details of the image. 2-D DCT is applied here for getting the DCT coefficients. Since, majority of the message information lies in the low-frequency parts of the DCT, so these components are preserved. The high-frequency coefficients contains noise, so these are altered in order to get the desired image. It is computed as:

$$DCT(m,n) = \beta_m \beta_n \sum_{p=1}^{X} \sum_{q=1}^{Y} I_{out}(p,q) cos \frac{\pi(2p+1)m}{2X} cos \frac{\pi(2q+1)n}{2Y} \tag{3}$$

where $1 \leqslant m \leqslant X$ and $1 \leqslant n \leqslant Y$. β_m and β_n are calculated as:

$$\beta_m = \begin{cases} \sqrt{\frac{1}{X}}, & m = 1 \\ \sqrt{\frac{2}{X}}, & \text{for } 2 \leqslant m \leqslant X \end{cases}$$

$$\beta_n = \begin{cases} \sqrt{\frac{1}{Y}}, & n = 1 \\ \sqrt{\frac{2}{Y}}, & \text{for } 2 \leqslant n \leqslant Y \end{cases}$$

After applying DCT on number of remote sensing test images we found that the maximum value lies in the upper left corner of the matrix i.e. DCT(1,1) and the maximum value corresponds to the maximum information. Therefore, we did not vary the DCT(1,1) component and rest all the coefficients are varied according to the equation below:

$$DCT'(m,n) = DCT(m,n)^{\gamma} \tag{4}$$

where DCT'(m,n) are the modified DCT coefficients. The above (4) applies for DCT(m,n) $>$ DCT(1,1). After this step final enhanced image ($I_{enhanced}$) is obtained by applying inverse 2-D DCT transform to the DCT'(m,n).

Algorithm 1 shows the pseudocode for the proposed method.

Algorithm 1 My algorithm.

I = *Input image*
L = *Maximum gray level=256*
I_{max}= *Maximum intensity of image*
I_{min}= *Minimum intensity of image*
Calculate the value of **Gamma**[γ]
Gamma(γ) = $\frac{Log(L)}{Log(I_{max}-I_{min})}$;
Calculate Histogram of image **I**
HIST[]:= Histogram of image
Find the no: of non zero bins of **HIST**
N = no: of non zero bins
Initialize M;
    for
    i = 1 to length(**N**)
    $M = [N(i) - I_{min}]^{\gamma}$;
    end
M will contain new values of image intensity
Now map the new intensity values to input image and calculate the modified image
Apply two dimensional discrete cosine transform (2-DCT) to the modified image
Adjust DCT coefficients
    $DCT'(image) = DCT(image)^{\gamma}$;
$DCT'(image)$= new DCT coefficients
Apply inverse DCT and obtain the final enhanced image

3.3 Impact of γ on image enhancement

The calculated value of γ is key adaptive parameter in our proposed method, since this directly effects on the enhancement results. Figure 4 shows the enhancement results of GF-1 image with different values of γ. It can be observed clearly that when γ value is less than 1, the image has become almost black and when γ is equal to 1, there is no enhancement. For calculated value of γ as in (2) the image contrast is enhanced very well with clear details. Again when γ value is much greater than 1 the image shows arte-facts.

Figure 5 shows the resultant transformation curve of two remote sensing images for different values of γ. Here x-axis shows the gray level of image and y-axis shows corresponding cumulative distribution function (CDF) at each gray level. Red curve shows the CDF for original image. Yellow curve shows CDF for the image when γ value is less than

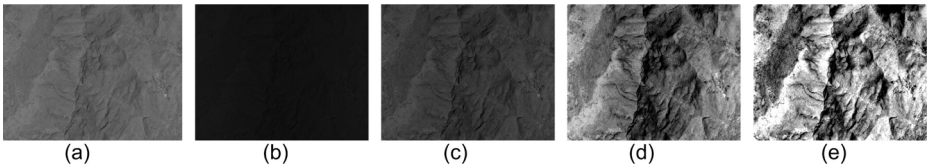

Fig. 4 Enhancement result of **a** Original **b** $\gamma < 1$ **c** $\gamma = 1$ **d** Calculated γ **e** $\gamma >> 1$

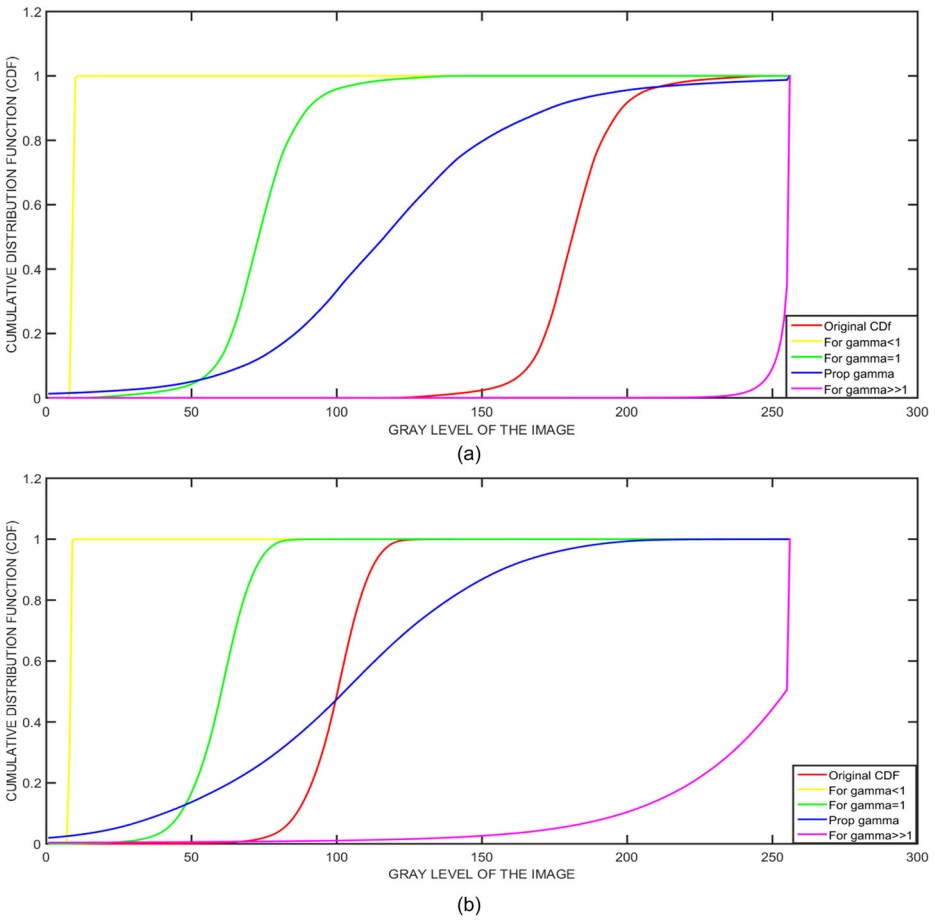

Fig. 5 Resultant transformation curve for different values of gamma(γ): **a** Transformation curve for Mars image, **b** Transformation curve for GF-1 image

1. Green curve shows CDF for the image when γ value is equal to 1. Blue curve shows CDF for proposed value of γ and magenta curve shows CDF for the image when γ value is much greater than 1. It can be clearly observe that for proposed γ value the mapping curve increases smoothly to the maximum value and this causes no over enhancement or distortion in the processed image, which is also clear from the Fig. 4.

4 Evaluation parameters

Quantitative assessment is a judgment of the numerical estimation of the image enhancement. In this paper four metrics are used for the analysis. The first is Discrete entropy (DE) [11]. Entropy is a count of randomness of the pixel intensities of an image. Entropy of an

image will be more if the pixels are more randomly distributed throughout the range. More entropy means more contrast of the image.

$$DE = -\sum_{i=0}^{L-1} p(I_i) log_2 p(I_i) \tag{5}$$

where $p(I_i)$ is the probability value of the i_{th} intensity level.

Second metric which is calculated here is measure of enhancement (EME) [1]. It gives the value that how much the processed image is enhanced in comparison to the original image. Consider an image f(x,y) be divided into k blocks $w_{m,l}(i, j)$ of sizes l1 x l2 and let ϕ be a known class of orthogonal transforms which is being used for image enhancement along with enhancement parameters then EME is defined as

$$EME(f) = EME\phi(f) = \frac{1}{k^2} \sum_{m=1}^{k} \sum_{l=1}^{k} 20 log_2 \frac{max(f[m,l])}{min(f[m,l])} \tag{6}$$

where $min(f[m,l])$ and $max(f[m,l])$ are respectively minimum and maximum of the image f(x,y) inside the block $w_{m,l}$.

Third parameter is Naturalness Image Quality Evaluator (NIQE) [8, 17]. It is a no-reference quality assessment metric. NIQE is dependent on statistical regularities that are obtained from natural and distortion free images. Basically, NIQE is constructed by accumulating of "quality aware" attributes and putting it to a multivariate Gaussian (MVG) model. The quality aware attributes are extracted by regular natural scene statistic (NSS) model. The quality score of any image is thereafter calculated by finding the distance of a MVG fit of the NSS attributes obtained from the test image, and a MVG model of the quality aware attributes obtained from the natural images.

$$D = \sqrt{\left((V_n - V_t)^T \left(\frac{M_n + M_t}{2}\right)^{-1} (V_n - V_t)\right)} \tag{7}$$

where V_n, V_t are the mean vectors and M_n , M_t are the co variance matrices of the natural MVG model and test image's MVG model respectively. NIQE value for an image should be as low as possible.

Histogram utilization efficiency (UE_{hist}) is another significant metric that can be calculated to interpret the property of the image histogram [18]. For a good contrast enhancement, the image must possess regularly scattered histogram throughout the complete area without changing the primary features of the histogram too much. UE_{hist} is given as:

$$UE_{hist} = \frac{NB_e}{NB_o} \tag{8}$$

where NB_e and NB_o represents the number of non-zero bins(utilized gray levels) of enhanced and original image correspondingly. Since, the number of non-zero bins in enhanced image is comparatively lower than original image the value of UE_{hist} is less than 1. But, if the value is much less than 1 it destroys the image quality. Hence, it should be closer to 1.

5 Results and analysis

This section describes the quantitative as well as visual results of the images. 24 satellite images were taken from the standard Computer vision group (CVG-UGR) database, 4 images were taken from [2] and 2 images were taken from [16]. In total 30 images were taken for test purpose.

5.1 Quantitative assessment

Table 1 shows the result of all four evaluation parameters for eight images. The best values are kept in bold. As we can observe from the table the entropy values obtained by the proposed method for Mars, GF-1, Sat1, Tank, Aerial, Truck, Aircraft and Surface images are 7.38, 7.41, 6.43, 6.80, 7.74, 7.45, 5.41 and 7.21 respectively which are highest values among all the other methods. Since, the original remote sensing image has very low contrast the entropy values for enhanced image should be more than the original image.

Next, if we analyze the EME values, proposed technique gives the highest values of EME for all the images. It shows that the proposed method results in maximum enhancement of the images.

NIQE should be as low as possible for an image. We can observe from the table that for our method NIQE values are lowest for all eight images.

From Table 1, it is noticed that UE_{hist} values for all the eight images is highest for our technique. From this it can be concluded that the proposed method can enhance the contrast very well together with preserving the basic features and characteristics of the image.

Figure 6 shows the average result for all the 30 images. Red line shows the result for EME. As it can be seen that proposed method gives the highest average EME. RHEDCT method gives the second highest average value for EME.

Blue line gives the result for entropy. Again, proposed method shows the highest average entropy and RHEDCT method second highest. PSO method is also very close to RHEDCT.

Green line shows the result for NIQE. Since, its value should be as low as possible, proposed method gives the lowest average value of NIQE among all the methods.

Violet line shows the result for UE_{hist}. Again, proposed method gives the highest average value of UE_{hist} as compared to other techniques.

Table 2 shows the result for computational complexity of different methods. It gives the average computation time in seconds. Result is shown for different sizes of images. As can be observed that proposed method requires least time to process the image. RHEDCT is also very close to proposed method. As discussed in the introduction section ACSEA and PSO methods have very high computational complexity, these two methods require highest time for processing an image.

5.2 Visual assessment

Visual assessment is the qualitative assessment of the images. Though this assessment is perspective in nature, but if the algorithm provides best visual look together with best quantitative values we can say that the image enhancement is appropriate.

Figure 7a has very low contrast. Figure 7b is the image obtained by DCTPSVD. Although the image has enhanced a bit but there are saturation and noise arte-facts. Figure 7c is the imaged obtained after applying AGCWD. The image is over enhanced and the details are lost in the bright portions. Figure 7d is the RHEDCT resultant image. It is well enhanced image but it still is has some noise issues. Figure 7e is obtained after applying ACSEA.

Table 1 Various parameters measures

Metric	Image	Original	DCTPSVD	AGCWD	RHEDCT	ACSEA	HCTLS	PSO	Proposed
Entropy	Mars	5.82	6.91	5.82	7.30	5.96	5.80	5.79	**7.38**
	GF-1	5.38	6.82	5.37	6.98	5.01	5.37	7.23	**7.41**
	Sat1	4.67	5.85	4.67	6.29	5.80	4.65	6.28	**6.43**
	Tank	5.87	6.27	5.78	6.66	5.64	5.80	6.70	**6.80**
	Aerial	6.38	6.97	6.02	7.22	6.42	6.50	7.01	**7.74**
	Truck	6.02	6.45	5.89	7.23	7.16	7.12	7.09	**7.45**
	Aircraft	4.00	4.02	4.87	5.01	4.46	4.43	4.93	**5.42**
	Surface	6.70	6.77	6.63	6.87	6.72	6.85	6.70	**7.21**
EME	Mars	3.92	11.56	3.92	14.56	6.54	11.35	5.32	**16.23**
	GF-1	7.19	10.98	7.35	12.97	6.54	10.85	11.65	**13.55**
	Sat1	7.11	9.82	7.20	12.38	7.15	9.12	10.43	**13.14**
	Tank	6.06	7.56	6.24	6.31	6.01	6.03	6.45	**9.01**
	Aerial	16.27	18.79	10.32	19.28	14.56	18.77	17.21	**19.45**
	Truck	10.81	12.67	6.78	15.79	11.66	12.23	11.87	**16.42**
	Aircraft	3.16	3.14	3.26	3.54	3.18	3.20	3.33	**3.74**
	Surface	9.75	10.11	7.65	12.34	9.84	10.98	9.75	**14.42**
NIQE	Mars	–	3.83	3.96	4.04	4.21	4.31	4.29	**3.61**
	GF-1	–	4.85	4.70	4.78	4.73	4.82	4.69	**4.66**
	Sat1	–	8.77	7.86	8.41	7.98	7.91	7.70	**7.56**
	Tank	–	3.12	3.02	2.65	2.75	2.97	2.87	**2.54**
	Aerial	–	2.48	4.98	2.41	3.46	2.46	2.39	**1.84**
	Truck	–	2.87	5.89	2.93	2.88	2.89	2.89	**2.84**
	Aircraft	–	5.68	5.87	4.53	5.32	5.16	5.77	**4.49**
	Surface	–	4.98	6.44	4.67	4.95	4.80	4.51	**4.64**
UE_{hist}	Mars	–	0.56	0.51	0.82	0.79	0.78	0.64	**0.87**
	GF-1	–	0.45	0.60	0.94	0.65	0.82	0.72	**0.97**
	Sat1	–	0.67	0.55	0.79	0.69	0.50	0.72	**0.80**
	Tank	–	0.77	0.63	0.73	0.52	0.76	0.68	**0.79**
	Aerial	–	0.64	0.45	0.83	0.70	0.78	0.85	**0.88**
	Truck	–	0.68	0.57	0.73	0.76	0.69	0.75	**0.81**
	Aircraft	–	0.52	0.76	0.82	0.72	0.78	0.68	**0.88**
	Surface	–	0.61	0.53	0.75	0.64	0.68	0.78	**0.79**

There is lot of noise in this image. Figure 7f is obtained by HCTLS. Visually seeing it is close to the proposed method but the image is not very much smooth. Figure 7g is the image obtained by applying PSO. Image is enhanced but is not visually appealing. Figure 7h is the enhanced image generated by our proposed technique. As we can observe that the image is very clear with all the global and local details highlighted.

Figure 8a is the original low contrast image. Again, we can observe that DCTPSVD generates noise and arte-facts in the image as seen in Fig. 8b. Figure 8c generated by AGCWD has saturation arte-fact in the white portions of the image and the details are not clear. Figure 8d has been globally enhanced by RHEDCT but the minute details of the image are not much highlighted. Figure 8e is obtained after applying ACSEA. It can be seen that image

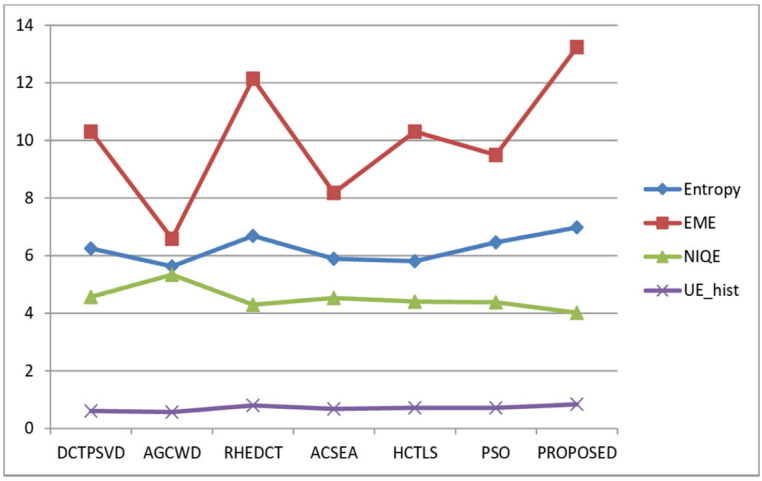

Fig. 6 Average result of 30 images for different methods

Table 2 Average computation time (in sec)

IMAGE SIZE	DCTPSVD	AGCWD	RHEDCT	ACSEA	HCTLS	PSO	Proposed
256x256	0.75	2.01	0.15	15.67	0.95	9.82	0.12
387x382	0.97	3.45	0.22	17.53	1.78	11.89	0.19
512x512	1.48	5.90	0.35	19.78	2.22	13.21	0.32
548x548	1.99	6.84	0.51	22.39	2.54	14.87	0.49
1500x1000	3.02	10.98	1.38	40.35	5.59	18.54	1.12

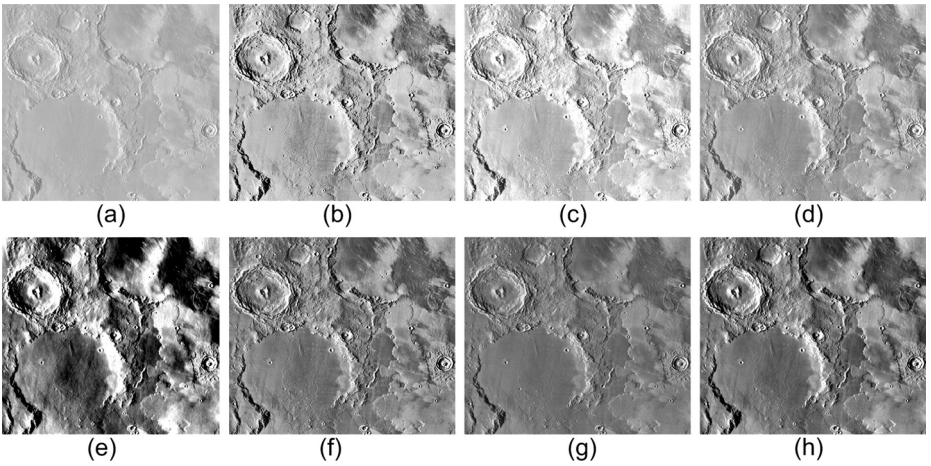

Fig. 7 Mars image: **a** ORIGINAL **b** DCTPSVD **c** AGCWD **d** RHEDCT **e** ACSEA **f** HCTLS **g** PSO **h** PROPOSED

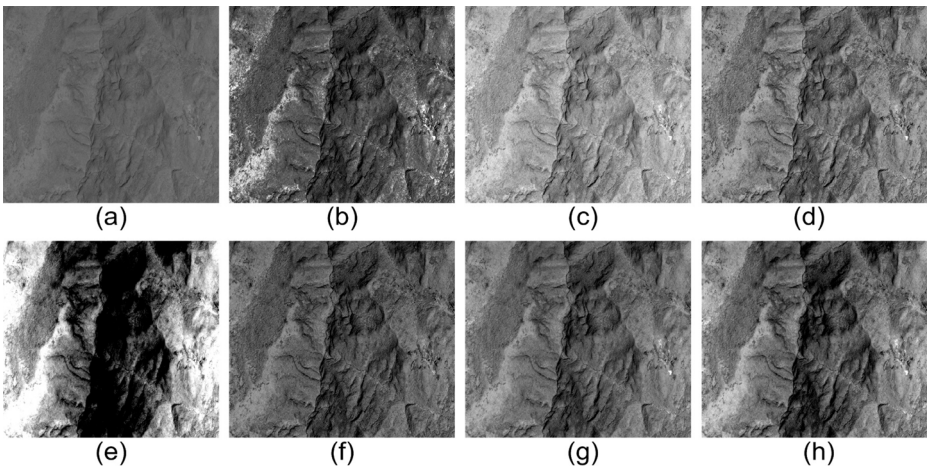

Fig. 8 GF-1 image: **a** ORIGINAL **b** DCTPSVD **c** AGCWD **d** RHEDCT **e** ACSEA **f** HCTLS **g** PSO **h** PROPOSED

has artefacts and also the details are lost. Figure 8f obtained by HCTLS is not enhanced well. Figure 8g is the resultant image of PSO. This image is very close to 8(d) image. Figure 8h contrast is enhanced very well by proposed method as well as details are very clear.

Figure 9 shows the result for Sat1 image. Image generated by DCTPSVD is well enhanced. AGCWD resulted in very bright image. RHEDCT showed very less enhancement for this particular image. Image obtained after applying ACSEA resulted in noise artefacts. HCTLS did not show enhancement for this image. PSO showed enhancement but again, it is not visually very appealing. Proposed method resulted in well enhanced image with clear details.

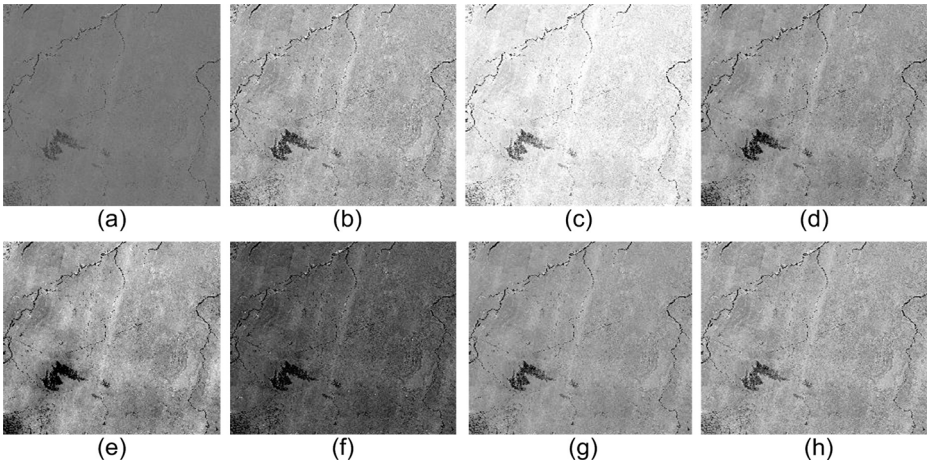

Fig. 9 Sat1 image: **a** ORIGINAL **b** DCTPSVD **c** AGCWD **d** RHEDCT **e** ACESA **f** HCTLS **g** PSO **h** PROPOSED

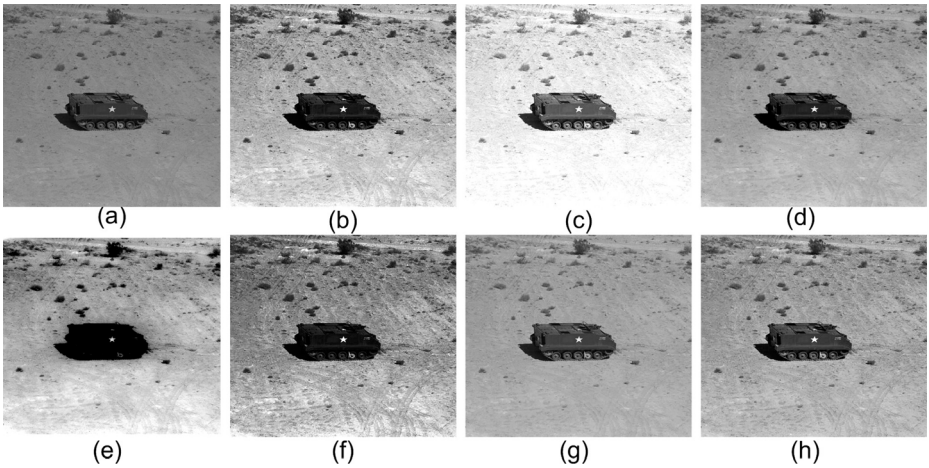

Fig. 10 Tank image: **a** ORIGINAL **b** DCTPSVD **c** AGCWD **d** RHEDCT **e** ACESA **f** HCTLS **g** PSO **h** PROPOSED

Figure 10 shows the result for Tank image. In Fig. 10 DCTPSVD, ACSEA and HCTLS methods generated noise in the enhanced image as can be seen in Fig. 10b, e and f. Figure 10c obtained by AGCWD had lost the details due to over enhancement. Figure 10d, g and h generated by RHEDCT, PSO and proposed technique provides well enhanced images, but Fig. 10h is much more clear with sharp details around the tank.

Figure 11 shows the result for Aerial image. In this figure AGCWD completely distorted the image. Images generated by DCTPSVD and HCTLS are almost similar. ACSEA resulted in over brightened image. RHEDCT and PSO techniques provided well enhanced images. Proposed method generated very clear image with sharp features and details.

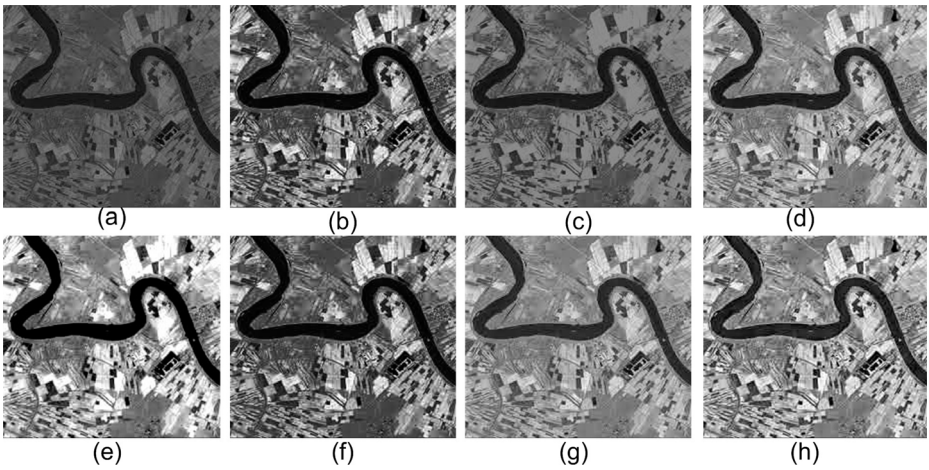

Fig. 11 Aerial image: **a** ORIGINAL **b** DCTPSVD **c** AGCWD **d** RHEDCT **e** ACESA **f** HCTLS **g** PSO **h** PROPOSED

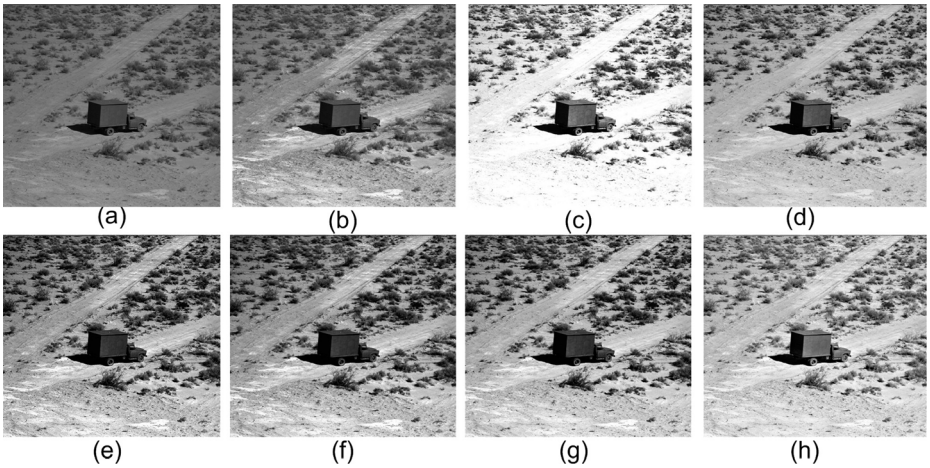

Fig. 12 Truck image: **a** ORIGINAL **b** DCTPSVD **c** AGCWD **d** RHEDCT **e** ACESA **f** HCTLS **g** PSO **h** PROPOSED

Figure 12 shows the result for Truck image. For this Figure we can observe that images generated by DCTPSVD, ACSEA, HCTLS and PSO are almost similar. These images are enhanced but are not very smooth. AGCWD again resulted in saturation artefact. RHEDCT enhanced the image well but proposed method generated more clear and smooth image.

Similarly Figs. 13 and 14 can also be analysed.

5.3 Noise estimation

Together with the qualitative and quantitative analysis of the images we also did the noise estimation [10] of the images. Figure 15 shows the noise analysis bar graph for the different

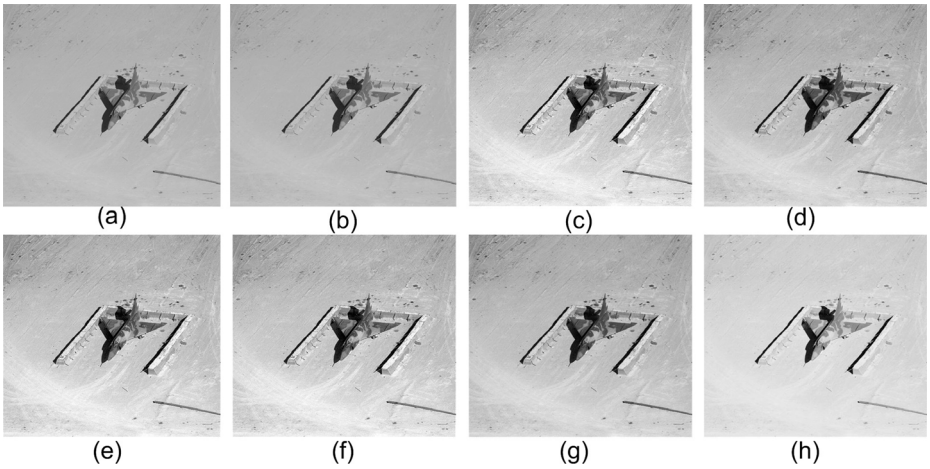

Fig. 13 Aircraft image: **a** ORIGINAL **b** DCTPSVD **c** AGCWD **d** RHEDCT **e** ACESA **f** HCTLS **g** PSO **h** PROPOSED

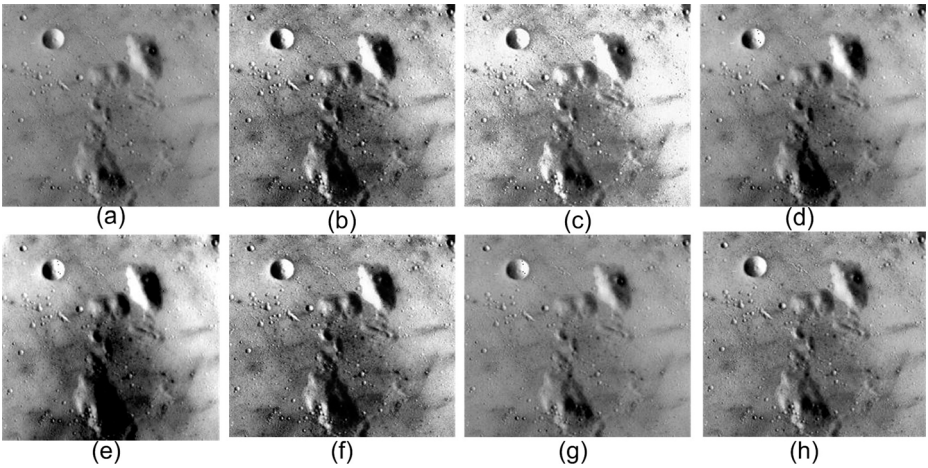

Fig. 14 Surface image: **a** ORIGINAL **b** DCTPSVD **c** AGCWD **d** RHEDCT **e** ACESA **f** HCTLS **g** PSO **h** PROPOSED

methods. As we can observe from the graph that for Figs. 10, 11, 12 and 13 the proposed method has the least noise generated in the enhanced image. For Fig. 7 PSO provided the least noise, for Figs. 8 and 9 HCTLS provided the least noise and for Fig. 14 PSO provided the least noise. Hence, we can say that proposed method provides best visual quality of an image while maintaining the noise input level in the image.

5.4 Enhancement of general images

Our proposed technique can also work very well for general standard test images. Figure 16 shows the result for two test images obtained from Computer vision group (CVG-UGR) database. Both the images contrast has enhanced very well as can be seen from the figure.

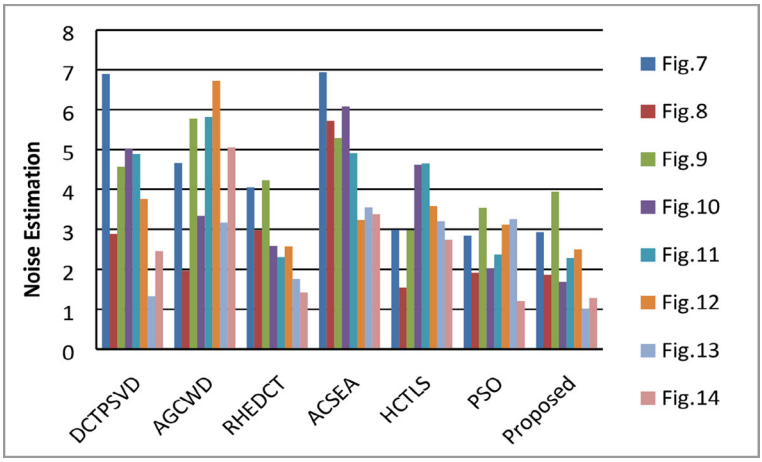

Fig. 15 Noise estimation with different methods

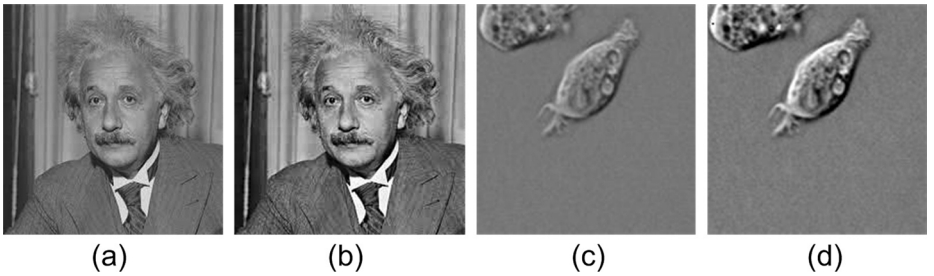

Fig. 16 Enhancement results: **a** Original Einstein image **b** Enhanced by proposed method **c** Original Cell image **d** Enhanced by proposed method

6 Conclusion

A new and efficient technique for remote sensing image enhancement is proposed in this paper. Adaptive gamma correction has been deployed for the global enhancement of the image and than the high frequency coefficients of the DCT transformation are modified in order to magnify the minute details of the previously enhanced image. Proposed method when compared to other state of the art papers visually resulted in superior quality of images. Quantitative assessment with the metrics like entropy, EME, NIQE and UE_{hist} also proved the supremacy of the proposed method. The computation complexity of the proposed algorithm is also much less as compared to other methods which makes it suitable to be used in real time applications.

Acknowledgements This work was supported by Dept. of Electronics and Communication Engineering, NIT Delhi.

References

1. Agaian SS, Lentz KP, Grigoryam AM (2000) A new measure of image enhancement. In: IASTED international conference on signal processing and communication
2. Atta R, Ghanbari M (2013) Low-contrast satellite images enhancement using discrete cosine transform pyramid and singular value decomposition. IET Image Process 7(5):472–483
3. Cao G, Zhao Y, Ni R, Li X (2014) Contrast enhancement-based forensics in digital images. IEEE Trans Inf Forens Secur 9(3):515–525
4. Celik T (2014) Spatial entropy-based global and local image contrast enhancement. IEEE Trans Image Process 23(12):5298–5308
5. Celik T, Tjahjadi T (2011) Contextual and variational contrast enhancement. IEEE Trans Image Process 20(12):3431–3441
6. Demirel H, Ozcinar C, Anbarjafari G (2010) Satellite image contrast enhancement using discrete wavelet transform and singular value decomposition. IEEE Geosci Remote Sens Lett 7(2):333–337
7. Fu X, Wang J, Zeng D, Huang Y, Ding X (2015) Remote sensing image enhancement using regularized-histogram equalization and DCT. IEEE Geosci Remote Sens Lett 12(11):2301–2305
8. Fu X, Zeng D, Huang Y, Liao Y, Ding X, Paisley J (2016) A fusion-based enhancing method for weakly illuminated images. Signal Process Elsevier 129:82–96
9. Huang SC, Cheng FC, Chiu YS (2013) Efficient contrast enhancement using adaptive gamma correction with weighting distribution. IEEE Trans Image Process 22(3):1032–1041
10. Immerker J (1996) Fast noise variance estimation. Comput Vis Image Underst 64(2):300–3012

11. Jang JH, Kim SD, Ra JB (2011) Enhancement of optical remote sensing images by sub band-decomposed multiscale retinex with hybrid intensity transfer function. IEEE Geosci Remote Sens Lett 8(5):983–987
12. Kallel F, Sahnoun M, Hamida AM, Chtourou K (2018) CT scan contrast enhancement using singular value decomposition and adaptive gamma correction. Signal Image Video Process 12(5):905–913
13. Kanmani M, Narsimhan V (2018) An image contrast enhancement algorithm for grayscale images using particle swarm optimization. Multimed Tools Appl 77(18):23371–23387
14. Kim Y (1997) Contrast enhancement using brightness preserving Bi histogram equalization. IEEE Trans Consum Electron 43(1):1–8
15. Lee E, Kim S, Kang W, Seo D, Paik J (2013) Contrast enhancement using dominant brightness level analysis and adaptive intensity transformation for remote sensing images. IEEE Geosci Remote Sens Lett 10(1):62–66
16. Liu J, Zhou C, Chen P, Kang C (2017) An efficient contrast enhancement method for remote sensing images. IEEE Geosci Remote Sens Lett 14(10):1715–1719
17. Mittal A, Soundararajan R, Bovik AC (2013) Making a completely blind image quality analyzer. IEEE Signal Process Lett 20(3):209–212
18. Parihar AS, Verma OP (2016) Contrast enhancement using entropy-based dynamic sub-histogram equalization. IET Image Process 10(11):799–808
19. Rahman S, Rahman MM, Wadud MAA, Quaderi GDA, Shoyaib M (2016) An adaptive gamma correction for image enhancement. EURASIP J Image Video Process 2016(35):1–13
20. Singh H, Kumar A, Balyan LK, Singh GK (2017) A novel optimally weighted framework of piecewise gamma corrected fractional order masking for satellite image enhancement. Comput Electr Eng, 1–17
21. Singh H, Kumar A, Balyan LK, Singh GK (2018) Slantlet filter-bank based satellite image enhancement using gamma corrected knee transformation. Int J Electron 105(10):1695–1715
22. Suresh S, Lal S, Reddy CS, Kiran MS (2017) A novel adaptive cuckoo search algorithm for contrast enhancement of satellite images. IEEE J Selected Topics Appl Earth Observ Remote Sens 10(8):3665–3676

Shubhi Kansal received the B.E. degree in Electronics and Communication engineering from R.G.P.V. in 2011. After that she pursued M.tech in VLSI Design from Banasthali Vidyapeeth, Rajasthan in 2013. Currently she is pursuing Ph.D from National Institute of Technology, Delhi. Her current research includes Image Enhancement in Image Processing, Image Segmentation.

Dr. Rajiv Kumar Tripathi received the B.E. degree in Electronics and Communication engineering from Agra University, 2002, M.Tech. degree in Digital Communication from U P Technical University, 2006, and completed his Ph.D. degree in Electrical Engineering from Indian Institute of Technology (IIT) , Kanpur in 2013. Presently working as Assistant Professor at National Institute of Technology, Delhi (NIT, Delhi) His current research interests lie in the area of Image Processing , Image Segmentation, Energy effcient routing and clustering in wireless sensor networks. Rajiv K. Tripathi is a member of the IEEE. He is Lifetime member of Institution of Communication Engineers and Information Technology, India.